Estimating global radiation at ground level from satellite images

Knut-Frode Dagestad

DOCTOR SCIENTIARUM THESIS IN METEOROLOGY
AT
UNIVERSITY OF BERGEN
MAY 2005

Preface

This synthesis and collection of papers constitute a thesis presented in partial fulfillment of the requirement for the degree of Doctor Scientiarum in meteorology at the Geophysical Institute, University of Bergen, Norway.

This thesis discusses the Heliosat algorithm which estimates solar radiation at ground level from satellite images. The performance of various versions of the algorithm has been analysed, and modifications are suggested.

Acknowledgments

First of all I want to thank my two supervisors, Arvid Skartveit and Jan Asle Olseth for excellent support and invaluable feedback.

This work is a part of the project "Heliosat-3", which has been funded by the European Commision. It has been a pleasure to work in the Heliosat-3 team, and the mood has always been humoristic and positive, despite that we were missing our satellite for a long time. A special thanks goes to the German colleagues Richard Müller, Rolf Kuhlemann and Hermann Mannstein who invited me to stay in their private homes during three of my stays in Germany.

I also want to thank all the staff and students at the Geophysical Institute for a very good working environment. In particular I want to mention Børge and Gard with whom I have shared my refrigerator and many enjoyable moments. I also want to mention Yngvar Gjessing for sharing some of his wisdom in many fields. Many thanks to Christiane and Frode for proofreading the thesis.

I am also very grateful to the Nansen Center for financially supporting this work the last nine months, and also for the very interesting new job which I am looking forward to do wholeheartedly from now on.

Finally, thanks to my family and friends for helping me having a somewhat normal social life (at least until recent months).

Bergen, May 2005 Knut-Frode Dagestad

Table of Contents

List of Papers

Paper I	Dagestad, K-F. (2004). Mean bias deviation of the Heliosat algorithm for varying cloud properties and sun-ground-satellite geometry. Theoretical and Applied Climatology, 79, 215–224.
Paper II	Müller, R. W., Dagestad, K-F., Ineichen, P., Schroedter, M., Cros, S., Dumortier, D., Kuhlemann, R., Olseth, J. A., Piernavieja, C., Reise, C., Wald, L. and Heinemann, D. (2004). Rethinking satellite based solar irradiance modelling - The SOLIS clear sky module. Remote Sensing of the Environment, 91, 160-174.
Paper III	Dagestad, K-F. and Olseth, J.A. (2005). An alternative algorithm for calculating the cloud index. Manuscript.
Paper IV	Dagestad, K-F. and Wald, L. (2005). Assessment of the database HelioClim-2 of hourly irradiance derived from satellite observations. Draft.
Paper V	Dagestad, K-F. (2005). Simulations of bidirectional reflectance of clouds with a 3D radiative transfer model. Manuscript.

1 Introduction

Every second the sun radiates more energy than people have used since the beginning of time. The amount of solar energy reaching earth is 1.76 x 10^{17} joules per second; more than 10000 times the global energy consumption today. Still this enormous source of energy accounts for only 0.1% of the total consumption, whereas 77% comes from fossil fuels (Worldwatch Institute 2003). The reasons for the low exploitation rate of solar energy are that it is difficult to collect since it is spread over the whole earth, and difficult to predict since it is fluctuating in time and space. To increase the efficiency of solar thermal power plants a detailed knowledge of the spatial and temporal variation of solar irradiance is needed. Such a climatology can be made by interpolating between measurement stations, as has been done in e.g. the European Solar Radiation Atlas, ESRA (Scharmer 1994). However, low spatial and temporal resolution of such data has led to nonoptimal site selection and incorrect system sizing, and thus unnecessary use of conventional energy sources.

Over the last two decades satellite-based retrieval of solar radiation at ground level has proven to be highly valuable for the solar energy community. With satellite pixel sizes of typically 2.5 kilometres, the spatial resolution of the estimates is much better than the data interpolated from ground measurements. It has also been found that for hourly values of global irradiance satellite retrievals are more accurate than interpolating ground measurements from stations which are more than 30 kilometres apart (Zelenka et al. 1999). However, the global markets for renewable energy sources such as solar and wind power are expected to see a dramatic expansion in the near future (Worldwatch Institute 2003), and there is a demand for solar radiation data of even higher quality. This can be made possible with more sophisticated satellite technologies and by improvement of the algorithms for conversion of satellite data into solar radiation data.

Heliosat is an algorithm which has been developed to estimate global horizontal irradiance at ground level from images taken in the visible range by the European meterological satellite series Meteosat. Starting with the launch of Meteosat-8 in August 2002 these satellites have now increased capabilities; the size of a pixel is now 1 kilometre, compared to 2.5 kilometres earlier, and the temporal resolution is increased from 2 to 4 images per hour. In addition, the number of spectral channels is increased from 3 to 12, making it possible to get a more accurate description of the atmospheric state. The work of this thesis deals with the improvement of the Heliosat algorithm, partly by taking advantage of the enhanced capabilities of the new generation of the Meteosat satellites.

The thesis is composed of two parts:

Part I provides an overview of the thesis. This introduction is the first chapter of this part. Chapter 2 gives an overview of the history of the Heliosat algorithm, and describes the various versions of the algorithm which are referred to later in the thesis. Section 2.4 discusses the prospects of Heliosat-3, the latest version which has been developed within the EU-project of the same name, based partly on the work of this thesis. Therefore this section also gives the objectives of the thesis. Chapter 3 discusses the concepts behind the Heliosat algorithm, and also gives an analysis of how sensitive the output of the algorithm is to some of its components. A summary of the five papers of the thesis is given in chapter 4 and concluding remarks are given in chapter 5.

Part II encompasses the five papers which constitute the main scientific work of the thesis.

2 History of the Heliosat algorithm

The first experimental weather satellite, TIROS-I, was launched by the USA in 1960. After several years of experiments the satellites were gradually improved and better adapted to their specific uses. 17 years later, in 1977, the European Space Agency launched Meteosat-1, the first satellite of the European meteorological satellite system. The main purpose of the Meteosat-satellites was to improve weather forecasts by giving the meteorologists a visual overview of the cloud cover on a global scale. In addition, several other applications of the satellite images quickly emerged; among them were methods to estimate the solar irradiance at ground level. However, the satellite data were very simple; each pixel of the images consisted of a digital count between 0 and 255, and these pixel counts could not even be reliably calibrated into radiances. Despite the input being simple, the output of these algorithms was surprisingly accurate when compared to ground measurements. The Heliosat algorithm, originally proposed by Cano et al. (1986), was one of the most popular algorithms because it was accurate and easy to implement (Grüter et al. 1986).

Heliosat was widely used in operational schemes around the world (Wald et al. 1992), and over the years it was modified several times. The naming of the different versions can be confusing, as a lot of versions exist with only minor differences from others. The following sections describe the versions which are referred to later in the papers of this thesis, and at the same time they give an overview of the major steps of the evolution of the Heliosat algorithm.

2.1 The original version

The first journal paper about the Heliosat algorithm was published in 1986 (Cano et al. 1986). This original version used uncalibrated counts of the Meteosat High Resolution Visible (HRV) sensor to calculate a reflectivity of the pixels:

$$\rho = \frac{C}{G_{clear}} \tag{1}$$

Here $\boldsymbol{C}$ is the digital counts of a pixel, an 8-bit number between 0 and 255, and $\boldsymbol{G_{clear}}$ is the clear sky global irradiance at ground level from an empirical model. The clear sky model in the first Heliosat scheme was very simple as it used only the solar elevation as input, and no information about the atmospheric turbidity at the given site. As a second step a ***cloud index n*** was calculated from a time series of reflectivities:

$$n = \frac{\rho - \rho_{clear}}{\rho_{cloud} - \rho_{clear}} \tag{2}$$

Here $\boldsymbol{\rho_{clear}}$ and $\boldsymbol{\rho_{cloud}}$ are the reflectivities corresponding to clear and overcast conditions, respectively. $\boldsymbol{\rho_{clear}}$ was decided by a histogram technique so that it is the "most frequent low reflectivity" of a given pixel for a given month. Similarly $\boldsymbol{\rho_{cloud}}$ was chosen as the "most frequent high reflectivity". A simple linear relation was then assumed between the cloud index and the ***clearness index*** $\boldsymbol{k_c}$:

$$k_c \equiv \frac{G}{G_{TOA}} = an + b \tag{3}$$

The clearness index is the ratio of the actual global irradiance, $\boldsymbol{G}$, to the irradiance at the top of the atmosphere, $\boldsymbol{G_{TOA}}$. The parameters $\boldsymbol{a}$ and $\boldsymbol{b}$ were tuned to ground measurements at a number of sites to minimise the deviation. Different values of the parameters were found for different sites and times of day, reflecting diurnal and spatial variation of atmospheric turbidity.

Although this scheme was very simple in its principle, implementation was relatively complex: the parameters ***a*** and ***b*** varied between the sites, and interpolation and extrapolation was done to provide global application. In some operational versions different values of these parameters were also used for morning, noon and afternoon. Consequently the accuracy was good at sites and times for which the constants ***a*** and ***b*** were tuned, and less good at sites where they were interpolated.

2.2 Heliosat-1

"Heliosat-1" refers in this thesis to the modified version of the algorithm which was developed within the EU-project "Satel-Light" (Fontoynont et al., 1998). This was the first operational large scale implementation of the algorithm, and global irradiance and derived products for the period 1996-2000 are disseminated for most of Europe on the web server www.satel-light.com. The main differences from the original version are described in Beyer et al. (1996), Fontoynont et al. (1998) and Hammer (2000):

- The reflectivity (ρ) is now calculated with:

$$\rho = \frac{C - C_{atm}}{G_{TOA}} \tag{4}$$

  The radiation scattered back to the satellite from atmospheric molecules, C_{atm}, is subtracted from the satellite measurements so that ρ is a reflectivity of the ground and clouds only. An empirical expression for C_{atm} was developed by Beyer et al. (1996) and later modified by Hammer (2000). The expression was tuned to digital counts of cloud free pixels over sea, assuming that the reflected radiance from the sea surface is negligible compared to the scattered radiance from air molecules.

  Instead of normalising with a modelled clear sky irradiance, the irradiance at the top of the atmosphere, G_{TOA}, is now used in the normalisation.

- The ***clearness index*** k_c (Equation 3) is replaced by the ***clear sky index k***, the actual global irradiance, ***G,*** divided by the output of a clear sky model, G_{clear}:

$$k \equiv \frac{G}{G_{clear}} \tag{5}$$

- In contrast to the relation between the cloud index and the clearness index (Equation 3) which had to be tuned to ground data at all sites, the relation between the cloud index and the clear sky index is now the same for any site. This new empirical relation is given by:

$$k = \begin{array}{ll} 1.2 & for\, n < -0.2 \\ 1 - n & for\, n \in [-0.2, 0.8] \\ 2.0667 - 3.6667\,n + 1.6667\,n^2 & for\, n \in [\ 0.8, 1.1] \\ 0.05 & for\, n > 1.1 \end{array} \tag{6}$$

The cloud index is still calculated with Equation 2.

In the original version the spatial and temporal variation of atmospheric turbidity was accounted for indirectly by tuning the parameters of the relation between the cloud index and the clearness index (Equation 3). In the Heliosat-1 version the atmospheric turbidity is a directly input parameter to the clear sky model. This is more convenient because such turbidity parameters are already available for other purposes, and they are also easier to interpret physically, in contrast to the parameters ***a*** and ***b*** of Equation 3.

The clear sky model used in the Satel-Light project consists of a model for the direct irradiance from Page (1996) and a model for the diffuse irradiance from Dumortier (1995). As input they used monthly values of Linke turbidities from a database developed by Dumortier (1998), height above sea level and solar elevation. The Linke turbidity coefficients are commonly used in meteorology, and account for the combined attenuation of broadband solar irradiance by aerosols and water vapour.

For the operational scheme an average of 3 pixels in the north-south direction and 5 pixels in the east-west direction was used, corresponding to a roughly square area in Europe where pixels are longer in the north-south direction due to the oblique viewing angle. The averaging led to better results, probably because the scale of this larger pixel-cluster better correlates the interval between subsequent images (30 minutes) with typical movement of clouds which are obstructing the path between the ground and the satellite sensor. Besides, this averaging is smoothing out the variability related to non-lambertian reflectivity, an issue which is discussed in Paper V of this thesis.

In Heliosat-1 the ground albedo was calculated separately for each slot (images acquired at the same time (UTC) of day belong to the same slot) for each month. This gave a better correlation with ground measurements, probably because the sun-ground-satellite configuration was kept fairly constant, thus minimising the effect of non-lambertian reflectivity.

2.3 Heliosat-2

Heliosat-2 uses the same principles as Heliosat-1, but a major difference is that calibrated radiances instead of raw digital counts are used as input (Rigollier et al. 2004). The HRV sensor of Meteosat is not calibrated routinely by Eumetsat, but a method for operational calibration was developed and used at Ecole de Mines in France (Lefevre et al. 2000, Rigollier et al. 2002). Heliosat-2 was also developed at Ecole des Mines, mainly during the EU-project SoDa from 2000-2001 (www.soda-is.com).

With calibrated radiances as input, Heliosat-2 uses the opportunity to replace some of the empirical parameters in the scheme with known physical/empirical models from external sources:

- The correction for the backscattered radiation from the atmosphere (Equation 4) is based on the ESRA clear sky model (Rigollier et al. 2000, Geiger et al. 2002). Here the clear sky diffuse irradiance is multiplied with a factor (empirical though) to convert the diffuse downwards irradiance to radiance upwards in the direction of the satellite.
- For calculation of the reflectivity, the ESRA clear sky model is used to calculate the transmissivity downwards to the ground and clouds and upwards to the satellite.
- An expression for the reflectivity of the thickest clouds is based on measurements from the Nimbus-7 satellite (Taylor & Stowe 1984).

No external physical model is used for the ground reflectivity, but rather second lowest value of the reflectivity of a time series for a given pixel. The extreme minimum is avoided because it can be due to artefacts in the processing of the satellite image. The relation between the cloud index and the clear sky index is the same as in the Heliosat-1 version (Equation 6). Thus, despite a physical calculation of the reflectivity, an empirical relation is still used to calculate the global irradiance from the cloud index.

2.4 Heliosat-3 (objectives of this thesis)

This thesis is a part of the EU-project "Heliosat-3", with the objective of further development of the Heliosat-algorithm to take advantage of the new generation of the Meteosat satellites. While the first seven Meteosat satellites (1977 until present) had only three spectral channels, the next generation (Meteosat Second Generation, MSG) has 12 spectral channels. When the project started in May 2001 the objective was to create an algorithm which in principle consisted of two steps:

1. The new spectral channels of the MSG-satellites should be used to acquire a thorough description of the atmospheric state for any pixel of any image:
   - clouds (optical depth, coverage, height, phase (water/rain), effective droplet size)
   - aerosols (type, single scattering albedo, optical depth)
   - water vapour amount
   - ozone amount
2. Given a description of the atmospheric state and the solar elevation, the global irradiance and other spectral and angular components should be calculated, preferentially with an advanced Radiative Transfer Model.

For the retrieval of the cloud properties, the scheme APOLLO (Saunders et al. 1988, Saunders 1988, Gesell 1989, Kriebel et al. 1989 and Kriebel et al. 2003) is adapted to the MSG satellites. APOLLO was originally developed for the AVHRR sensor of the NOAA satellites, but adaptation to MSG was performed within the project by the German Remote Sensing Data Center (Deutsche Zentrum für Luft und Raumfahrt, DLR), one of partners of the Heliosat-3 consortium.

However, the launch of the first of the MSG-satellites was delayed from October 2000 until 28 August 2002. Furthermore, a power supply switched off unexpectedly in October 2002, resulting in even more delay of the operation. Following was a period of commissioning and validation by Eumetsat, and subsequently implementation of the APOLLO algorithm by DLR. Consequently the APOLLO derived cloud parameters were not available for development of a new scheme until after the official end of the project in May 2004. However, the EU extended the project until February 2005, but within the remaining time no improvement of the Heliosat algorithm was achieved by integrating the cloud products in the scheme.

Anticipating the delay of data from MSG, the objective within the project was modified to improve the Heliosat-1 scheme based on the calculation of a cloud index. The Heliosat-3 project also deals with the calculation of other solar radiance component like splitting into direct and diffuse radiation, and splitting into spectral components like Ultraviolet, Photosynthetically Active Radiation, Solar Cell Response and Luminance/Illuminance, but this thesis is focusing mainly on the calculation of the horizontal global irradiance.

The main objectives of this thesis are then:

- To develop a clear sky model which can use the operationally retrieved values of aerosols, water vapour and ozone as input. By replacing the simple empirical models used earlier with a numerical Radiative Transfer Model it will also be possible to have spectral output which will ease the subsequent calculation of spectral radiative parameters.
- To improve the calculation of the cloud index with respect to the following points:
  - It should be based more on general physical principles and less on tuned empirical parameters. This will ensure that the scheme will also work well for conditions different from those where the tuning has taken place.
  - It should be as fast and easy to implement as possible for use in an operational scheme.
- To assess the uncertainty related to sub-pixel variability of the cloud properties. A 3D

Radiative Transfer Model will be used to give advice on the ideal size of a pixel and possibly also to suggest modifications to the scheme.

- In general to improve the accuracy of the calculation of global irradiance, both on a short term but also on longer terms by building the algorithm on physical principles. The algorithm will then be easier to interpret/understand for further development.

3 The concepts of the Heliosat algorithm

Like radiation itself, the Heliosat algorithm has a dualistic nature. It can be interpreted as a physcal algorithm, based on the equation for conservation of energy. However, it can also be interpreted as a very simple empirical algorithm, which seems to work well mainly due to statistical cancelling of errors. A very simple - perhaps naive - interpretation of the Heliosat algorithm is given in section 3.1, and in section 3.2 a more strict physical interpretation follows. Section 3.3 is an analysis of how sensitive the output of Heliosat is to the choice of the parameters $\boldsymbol{\rho}_{clear}$ and $\boldsymbol{\rho}_{cloud}$ (Equation 2).

3.1 An empirical approach

A simple interpretation of the Heliosat algorithm is the following:

1. The reflectivity of a Meteosat pixel is calculated by normalising the raw digital counts with incoming radiation at the top of the atmosphere.
2. From a time series the "typical lowest and highest reflectivities" are identified.
3. When the reflectivity is equal to the lowest value the irradiance at ground equals the output of an empirical clear sky model.
4. When the reflectivity is equal to the highest value the irradiance at ground is estimated to be zero.
5. For intermediate reflectivity the irradiance is linearly interpolated between zero and the clear sky value.

Some corrections are then added to these simple principles:

- The scattered radiation from air molecules is subtracted from the normalised digital counts with an empirical formula. This makes the reflectivity more lambertian, at least for the clear sky case, and hence it is easier to compare reflectivities measured under different sun-ground-satellite geometries.
- Empirical experience tells us that even under the thickest cloud cover it is never completely dark. When the reflectivity is close to the "typical highest reflectivity" the global irradiance is therefore increased to ca 5-10% of the clear sky value.
- It is found that by averaging the reflectivity over 3x5 pixels the accuracy of the algorithm is higher when compared to ground measurements.

3.2 A physical approach

Conservation of energy implies that solar radiation reaching the top of the atmosphere can be either:

1. reflected to space,
2. absorbed in the atmosphere or
3. absorbed in the ground.

In the general case this can be expressed as:

$$I = R + G(1-\alpha) + A \quad (7)$$

where

- I is the incoming irradiance at the top of the atmosphere
- R is the irradiance reflected to space
- G is the irradiance reaching the ground (global irradiance)
- α is the ground albedo
- A is the radiation absorbed in the atmosphere

In the case of no clouds or overcast we have, respectively:

$$I = R_{clear} + G_{clear}(1-\alpha) + A_{clear} \quad (8)$$

and

$$I = R_{cloud} + G_{cloud}(1-\alpha) + A_{cloud} \quad (9)$$

For these cases 'clear' and 'cloudy' atmospheres have to be defined for a reference.

By neglecting the atmospheric backscatter correction used in Heliosat-1 and Heliosat-2 (Equation 4), and assuming isotropic reflection in all cases, the calculation of the cloud index (Equation 2) is equivalent with:

$$n = \frac{R - R_{clear}}{R_{cloud} - R_{clear}} \quad (10)$$

where radiances have been replaced by irradiances. Solving for these irradiances in Equations 7-9 and inserting into Equation 10 gives:

$$n = \frac{(1-\alpha)(G_{clear} - G) + A_{clear} - A}{(1-\alpha)(G_{clear} - G_{cloud}) + A_{clear} - A_{cloud}} \quad (11)$$

Solving again for the global radiation ***G*** in the general case and introducing the ***clear sky index k*** gives:

$$k \equiv \frac{G}{G_{clear}} = 1 - n + \frac{G_{cloud}}{G_{clear}} n + \frac{n(A_{cloud} - A_{clear}) + A_{clear} - A}{(1-\alpha) G_{clear}} \quad (12)$$

By neglecting the variation of atmospheric absorptance ($A = A_{clear} = A_{cloud}$) this reduces to:

$$k = 1 - n + \frac{G_{cloud}}{G_{clear}} n \quad (13)$$

A typical value for the ratio G_{cloud}/G_{clear} is 0.1, but it depends on the solar elevation and the choice of the reference cloud. Equation 13 is not identical to the empirical relation which has been tuned for best performance of the actual Heliosat algorithm (Equation 6), but there are also several differences between the "real world" and this idealised version:

- Reflectivities are not generally lambertian.

- A correction for the backscattered radiation from air molecules is used in Heliosat.
- The absorptance in the atmosphere varies with solar elevation, cloudiness and turbidity.
- The Meteosat HRV sensor does not measure broadband radiances but is limited to 0.45-1.0 micrometres.
- Heliosat is tuned to give best correlation between estimated global irradiance averaged over an area (satellite pixel) at a single point in time, and measured global irradiance at ground at a single spot but averaged in time.
- The theoretical model considers an atmosphere which is homogeneous in the horizontal direction. In reality there are large variations, especially of cloud properties. Thus the empirical relations implicitly account for effects like reduced irradiance due to shadows from nearby clouds, and enhanced radiation due to scattered radiation from broken clouds.
- The broadband ground albedo $\boldsymbol{\alpha}$ will change slightly when the spectral variation of the incoming irradiance is changing due to varying atmospheric conditions and solar elevation.

3.3 A sensitivity analysis

Whether Heliosat is interpreted physically or empirically, the definitions of the reference reflectivities for clear and overcast conditions (ρ_{clear} and ρ_{cloud}, respectively) are vital. In the various versions of the Heliosat algorithm these parameters are calculated in different ways:

- In the original version of the Heliosat algorithm (Cano et al. 1986) ρ_{clear} and ρ_{cloud} were defined as the "most typical values of the reflectivity for clear and overcast conditions". These values were calculated from a time series of the reflectivities with a histogram technique to find the most frequent high and low values from the typical bi-modal distribution.
- In Heliosat-1 the parameter ρ_{cloud} was set to the constant of 160 normalised digital counts for all pixels (Hammer 2000). This value was chosen as the 96 percentile of a time series of all the reflectivity values for the whole field of view of Meteosat.
- In Heliosat-2 an external empirical model was used for ρ_{cloud} since calibrated radiances were used as input instead of uncalibrated digital counts, whereas the parameter ρ_{clear} was taken as the second lowest value of a time series.

For consistency with Equation 6, a stringent definition of ρ_{clear} should be "the reflectivity for which the global irradiance at ground is equal to the clear sky model". Similarly the definition of ρ_{cloud} should be "the reflectivity for which the global irradiance at ground is equal to 6.7% of the clear sky model (Equation 6 evaluated at n=1)"

The global irradiance calculated with Heliosat is given by Equation 5, which can be written as:

$$G = G_{clear}\, k(n) \tag{14}$$

It is obvious from this equation that the error of the estimated global irradiance is proportional to the error of the clear sky model. Thus an accurate clear sky model is vital. The sensitivity of the estimated global irradiance to the parameter ρ_{clear} can be found by differentiating Equation 14:

$$\frac{dG}{d\rho_{clear}} = G_{clear} \frac{dk}{dn} \frac{\partial n}{\partial \rho_{clear}} \tag{15}$$

The relative sensitivity is given by:

$$\frac{1}{G}\frac{dG}{d\rho_{clear}} = \frac{1}{k(n)}\frac{dk}{dn}\frac{\partial n}{\partial \rho_{clear}} \tag{16}$$

Assuming first a simple relationship ***k = 1 - n***, Equations 15 and 16 become, respectively:

$$\frac{dG}{d\rho_{clear}} = G_{clear}\frac{\rho_{cloud} - \rho}{(\rho_{cloud} - \rho_{clear})^2} \tag{17}$$

and

$$\frac{1}{G}\frac{dG}{d\rho_{clear}} = \frac{1}{\rho_{cloud} - \rho_{clear}} \tag{18}$$

For the parameter $\boldsymbol{\rho_{cloud}}$ the corresponding absolute and relative sensitivities are, respectively:

$$\frac{dG}{d\rho_{cloud}} = G_{clear}\frac{\rho - \rho_{clear}}{(\rho_{cloud} - \rho_{clear})^2} \tag{19}$$

and

$$\frac{1}{G}\frac{dG}{d\rho_{cloud}} = \frac{\rho - \rho_{clear}}{(\rho_{cloud} - \rho_{clear})(\rho_{cloud} - \rho)} \tag{20}$$

Figure 1 shows the sensitivities from Equations 17, 18, 19 and 20 plotted versus the cloud index for typical values of $\boldsymbol{\rho_{clear}}$ and $\boldsymbol{\rho_{cloud}}$ of 0.2 and 0.8 respectively. On the upper part of the figure one can see that the estimated global irradiance is most sensitive to $\boldsymbol{\rho_{clear}}$ for clear cases and to $\boldsymbol{\rho_{cloud}}$ for cloudy cases. The magnitude is, however, equal: a 0.01 too high value of $\boldsymbol{\rho_{clear}}$ will give an overestimation of global irradiance by almost 2 percent of the clear sky values for clear cases, and a 0.01 too high value of $\boldsymbol{\rho_{cloud}}$ will give the same overestimation of global irradiance for the cloudy cases. Hence if one assumes equally many clear and cloudy cases, the average bias of the Heliosat algorithm is equally sensitive to both parameters. However, since the irradiance is lower for the cloudy cases, the relative bias for the cloudy cases is much higher, as seen on the lower part of Figure 1.

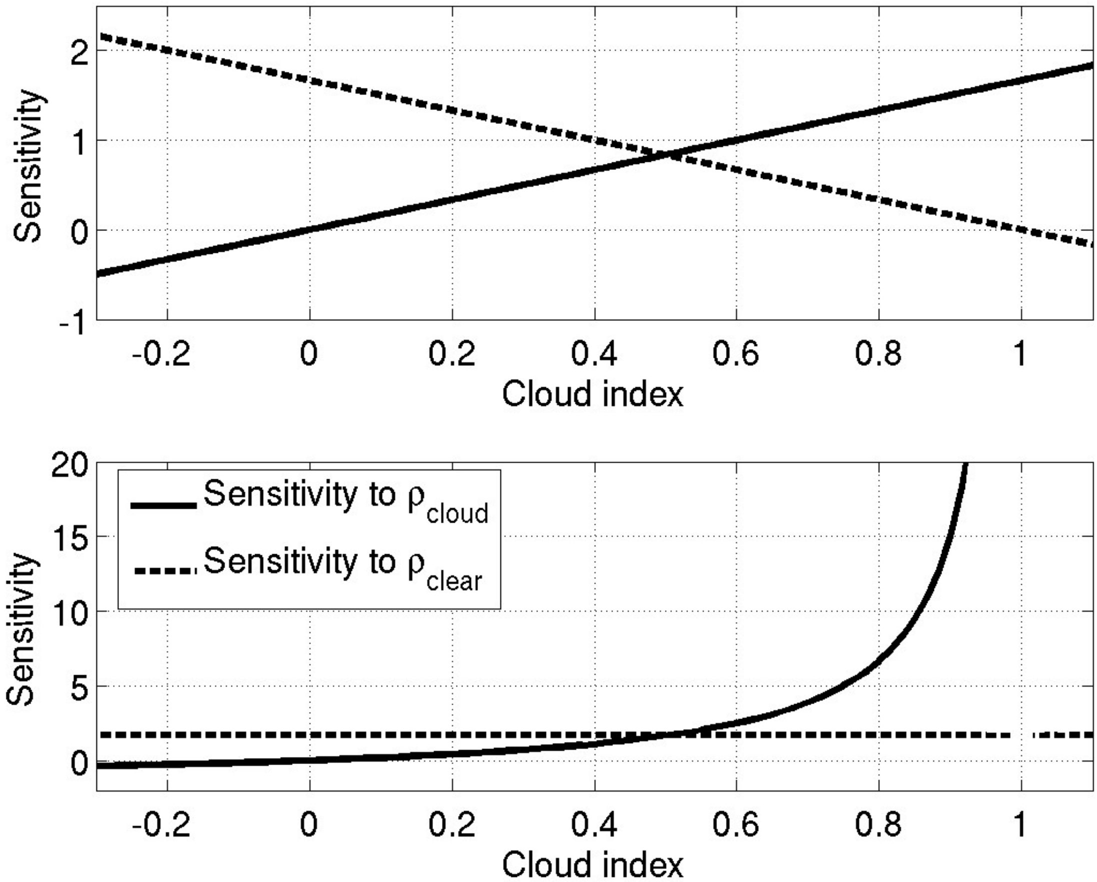

Figure 1: Sensitivity to the parameters ρ_{clear} and ρ_{cloud} of the global irradiance estimated with the Heliosat-algorithm. Values of 0.2 and 0.8 are used for ρ_{clear} and ρ_{cloud} respectively. The upper figure shows the change, in units of the clear sky irradiance G_{clear}, resulting from a unit change of the parameters ρ_{clear} and ρ_{cloud}. This is calculated with equations 17 and 19, respectively. The lower figure shows the same, but the unit of change is the fraction of the actual estimated irradiance. This is calculated with equations 18 and 20.

Figure 2 shows the sensitivities using the relation between the clear sky index and the cloud index which is used in Heliosat-1 and Heliosat-2 (Equation 6). The relative sensitivity to the parameter $\boldsymbol{\rho_{cloud}}$ is now not singular for a cloud index of one, as it is for the simple relation $\boldsymbol{k=1-n}$. However, the lower part of the figure shows that a value of $\boldsymbol{\rho_{cloud}}$ which is too large by only 0.01 will lead to an overestimation of the global irradiance by almost 10 percent for the cloudy cases.

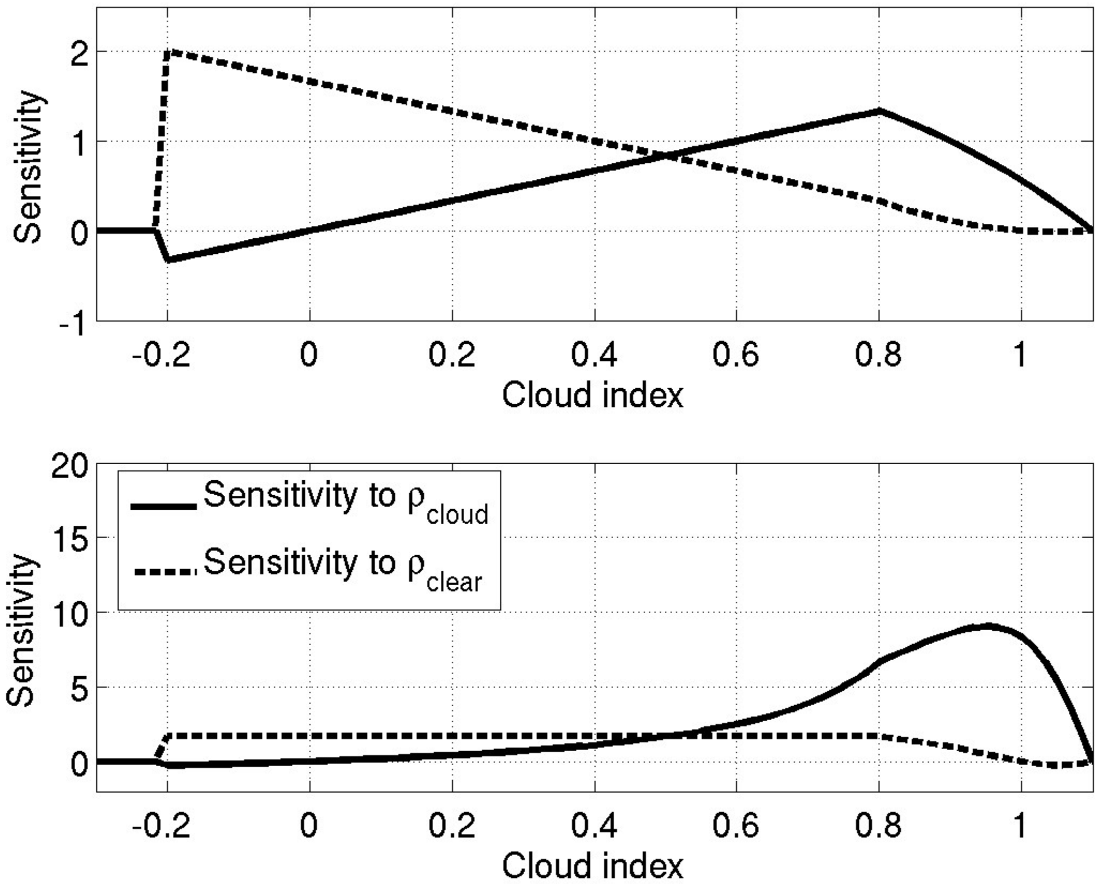

Figure 2: Same as Figure 1, but the relationship between the clear sky index and the cloud index is given by equation 6 from Fontoynont et al. (1998). The new equations corresponding to equations 17, 18, 19 and 20 are not shown in the text.

4 Summary of results

4.1 Paper I

The first paper is mainly a validation of the Satel-Light version of the Heliosat-algorithm (section 2.2). The objective of this work was to identify how well the algorithm is working for various situations and from that find out how it can be improved. To investigate the influence of the sun-ground-satellite geometry, the performance of the algorithm was analysed for variations of the three angles shown on Figure 3.

For overcast situations Heliosat gave too high solar irradiance for low sun and too low irradiance for high sun. For clear situations there were no such biases. In Heliosat there is an implicit assumption that the variation of solar irradiance with solar elevation is similar for clear and cloudy cases. However, numerical simulations with a radiative transfer model showed that irradiance at ground is decreasing faster with solar zenith angle for overcast conditions than for clear conditions. A semi-empirical correction for this was suggested.

The deviation between satellite estimates and ground measurements also depends on the solar azimuth angle (or time of day), but much of this variation can be explained by the correlation between the azimuth angle and the solar zenith angle. However, for Bergen it was found that while the modelled global irradiances were symmetric around noon, the measurements were higher in afternoon than in the morning. This asymmetry was only found for intermediate cloudiness, thus suggesting an explanation: even though the average cloudiness did not change with time of day, the scattered clouds were more likely to be positioned over land (to the east) than over sea (to the west). Thus there is greater chance that a given cloud fraction will make shadows at the pyranometer in the morning than in the afternoon. Heliosat relies on the hypothesis that clouds are randomly placed within a pixel, but this "frozen turbulence hypothesis" seems to be violated for Bergen. Empirical corrections for this phenomenon can easily be implemented for a particular site like Bergen, but a general correction is impossible without knowledge of the local conditions for each pixel.

The bias is also seen to depend strongly on the co-scattering angle ψ (Figure 3), but again most of this is seen to be due to the correlation with solar zenith angle. When this correlation is corrected for, the opposition effect is seen: when the sun and the satellite are in the same direction (ψ is close to zero) less shadow is seen, and hence the reflectivity is higher. This gives a higher cloud index, and thus the global irradiance is underestimated.

The performance of Heliosat was also analysed in light of the total cloud cover and the height of the base of the lowest clouds, as estimated from human observers at ground. For Bergen it was seen that for overcast situations the observed irradiance was smaller than the modelled irradiance. A possible explanation for this is that the clouds in Bergen are very thick, something which also is found by Leontieva et al. (1994). A correction for this can be possible with the second generation of Meteosat satellites (MSG), from which cloud optical thickness can be retrieved by use of more spectral channels. It was also found that Heliosat overestimated global irradiance when the observed height of the cloud bases was very low. Numerical simulations with a radiative transfer model suggest an explanation: by increasing the height of the clouds, the irradiance reaching ground is constant, while the increased reflection is perfectly matched by a decrease of radiation absorbed in the atmosphere. With the MSG satellites cloud (top) height will also become available, and hence a correction for the influence of the cloud height can be implemented.

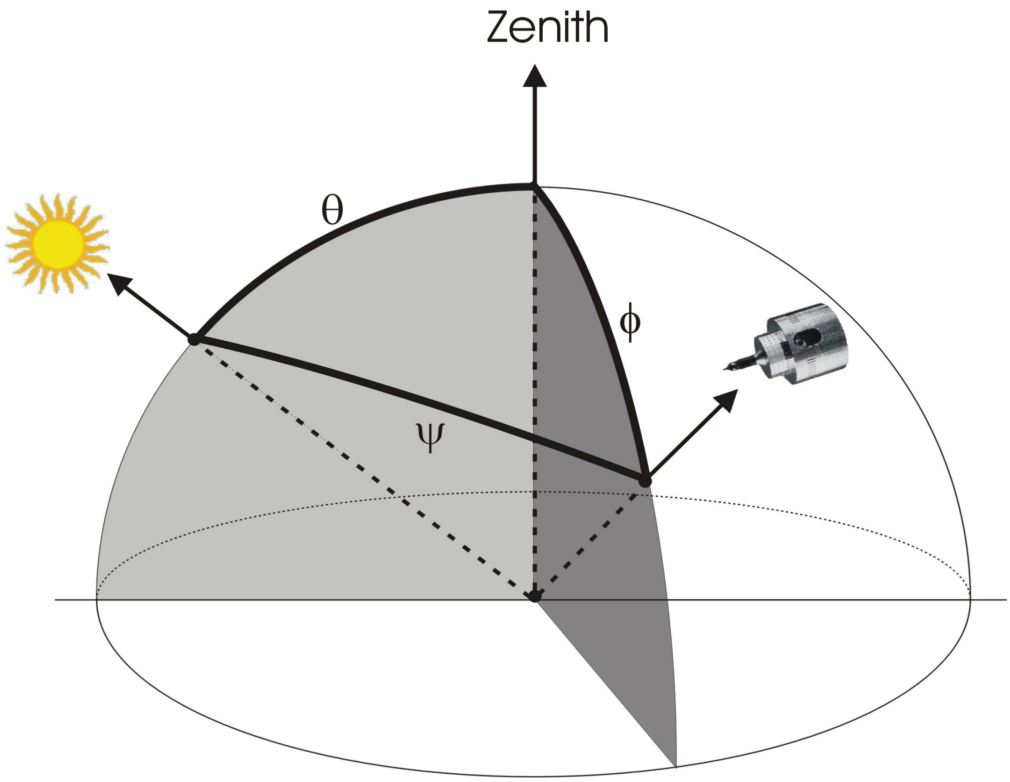

Figure 3: The three angles which are used in this thesis to describe the sun-ground-satellite configuration: solar zenith angle (θ), satellite zenith angle (ϕ) and co-scattering angle (ψ).

4.2 Paper II

One of the objectives of the Heliosat-3 project was to include a Radiative Transfer Model (RTM) directly into the scheme. The advantage of using an RTM is that it can take more detailed input data than the simple models used earlier, and that it can produce spectral output in addition to integrated broadband irradiances. However, it will be unrealistic to run an RTM for each pixel in each image. With approximately 2.5 million pixels to be processed for each image, and an RTM runtime of typically 5 seconds, it would take approximately 3500 hours to process one image. Since MSG produces one image every 15 minutes this approach can not be used in an operational scheme, even with the fastest computers available. Paper II introduces a workaround solution to this problem: an RTM will be used for the clear sky calculations only, and with a spatial resolution of 100 times 100 kilometres. This reduces the runtime to a manageable length, while keeping adequate resolution to describe the spatial variation of atmospheric turbidity. The full resolution will only be used for calculating cloud parameters, which will then be combined with the clear sky calculations with a simple empirical relationship to estimate the radiation at ground. The cloud parameters can then be the traditional cloud index, but also the more physical cloud parameters retrieved with the APOLLO scheme. The paper demonstrates that it is sufficient with two model runs per pixel per day, and that the diurnal variation of the clear sky irradiance can be parameterised with the output from the two model runs. Paper II was mainly written by the first author, Richard Müller. My contribution was discussion and development of the concept of how to reduce the necessary number of runs with an RTM, during a stay in Oldenburg, during project meetings and by email. I also wrote section 4.3 of the paper, a validation of the scheme using daily values of ozone and water vapour and climatological values of aerosol type and optical depth.

4.3 Paper III

This paper presents two modifications to the algorithm which is used to calculate the cloud index.

The first modification concerns the backscatter correction in the Heliosat scheme (Equation 4). In the calculation of the cloud index the part of the satellite signal that is scattered from the atmospheric molecules is subtracted. This correction was introduced by Beyer et al. (1996), and an empirical expression was developed. By assuming that the reflected radiance from the sea surface is negligible to the contribution scattered from the air molecules, Beyer et al. fitted an expression to the count values of Meteosat HRV images for a number of cloud free pixels over sea in Western Europe for August 1993. In Hammer (2000) this expression was modified by fitting to a larger database. Paper III of this thesis replaces these empirical expressions with an analytical expression. This is possible by assuming a plane-parallel atmosphere and that multiple scattering is negligible for the wavelengths of the satellite sensor. The expression is derived for monochromatic radiation, but it is demonstrated that by use of an "equivalent wavelength" it is not necessary to perform integration over the spectral region of the sensor. While the empirical expressions used earlier are tuned for a particular satellite sensor, the new analytical expression can easily be adapted to other sensors. Furthermore, while the empirical equations are fitted to certain sun-ground-satellite configurations (Figure 3), the new expression is valid for all angles for which the plane-parallel approximation is reasonable.

The second modification concerns the calculation of the reflectivity of the ground for each pixel. In earlier versions of Heliosat this parameter (ρ_{clear}) was determined for each month and each slot. This assures that the sun-ground-satellite geometry is fairly constant, and therefore avoids partly the problem of non-lambertian reflection. However, this is a time consuming part of the algorithm, and besides it can be difficult to determine ρ_{clear} for months and slots with few clear situations. In Paper III it is demonstrated that the lower bound of reflectivity can be parameterised with the co-scattering angle (ψ on Figure 3). Thus the ground albedo for each pixel can be calculated once and for all, and the algorithm will then be significantly faster and simpler to implement.

Global irradiances are calculated using both the modified cloud index from this paper and the traditional cloud index from the Heliosat-1 version (Section 2.2). Two different clear sky models are also used for the calculations: the model from Heliosat-1 and the new SOLIS model developed in Paper II, both using climatological input of turbidity data. When compared to ground measurements at five European stations, it is found that the accuracy is quite similar for all of the four combinations of the two cloud indices and the two clear sky models. However, it is found that the new cloud index is on the average higher than the traditional one, particularly for low values as it is less frequently negative, and that the SOLIS model gives generally lower clear sky values than the traditional clear sky model. Consequently the new cloud index gives best results when combined with the old clear sky model, and vice versa. It is therefore important to be aware of this when combining a cloud index with a clear sky model in the Heliosat scheme.

4.4 Paper IV

Paper IV gives a validation of the database HelioClim-2, which provides global irradiance for the solar energy and daylight community on the internet. The HelioClim-2 data is calculated with the Heliosat-2 algorithm (section 2.3) using Meteosat images which are sampled in both time and space as input. The sampling is done to be able to efficiently process long time series of data for the whole field of view of Meteosat for climatological purposes. In this paper five European ground stations are used for the comparison.

For daily values of global irradiance HelioClim-2 performs much better than the previous version of the database (HelioClim-1) which used a lower sampling frequency in both time and space. However, HelioClim-2 gives a larger Root Mean Square Deviation than Heliosat-1 (section 2.2). Most of this difference is probably due to the sampling of the satellite data, but some of it can also be due to differences between the Heliosat-1 and Heliosat-2 algorithms.

HelioClim-2 overestimates the global irradiance for all five ground stations, and for the station Bergen the bias is as large as 21%. Since there are also more cloudy cases in Bergen than for the other sites, it is suggested that Heliosat-2 overestimates the global irradiance for the cloudy cases. It is shown that this overestimation can be due to a too high value for the cloud reflectivity.

This paper is a draft only. The second author, Lucien Wald, will later conclude the paper with a discussion of the effects of interpolating and sampling the satellite data which are input to HelioClim-2. Besides, HelioClim-2 will be reprocessed with a lower value of the cloud reflectivity, as suggested in the draft, to see if the bias will be smaller.

4.5 Paper V

The greatest challenge of the Heliosat algorithm is that cloud properties are varying on a scale which is often smaller than the size of the satellite pixels. This sub-pixel variability cannot be accounted for directly, since detailed information is missing. Nevertheless it is of interest to have an estimate of the variability of the reflected radiance for different sizes of the pixels. In this paper a 3-dimensional radiative transfer model, SHDOM, is used to simulate the reflectance towards a satellite from two different cloud fields. One is a rather homogeneous stratocumulus field, but with typical 'bumps' on the top, and the second is a broken cumulus field with only scattered clouds. With the sun and 'satellite' in fixed positions, the cloud fields are rotated in the azimuth direction. It is found that by observing the full stratocumulus field of 3520 metres, there is no variation of the reflectance. For the cumulus cloud field the variability is approximately 10-20 percent, even though the size of this field is larger; 6700 metres. Looking at smaller subsets of the cumulus cloud field, the variability is extreme, while for the stratocumulus field it is more moderate.

In Paper V the distribution of reflected radiance from the stratocumulus field in different directions is also compared with reflectances measured with Meteosat. When plotted versus the co-scattering angle (ψ on Figure 3) it is found that the reflectance of the thickest clouds measured with Meteosat is rather homogeneous, but with a minimum around ψ = 60 degrees. The simulated reflectances depend on ψ in a qualitatively similar way, but the variation is much larger: the reflectivity for ψ = 60 degrees is only 50 percent of the reflectivity for ψ close to zero (i.e. when the sun and the satellite are in the same direction, as seen from the cloud field). One of the objectives of this study was to find a parameterization of ρ_{cloud}, the albedo of the thickest cloud used in Heliosat. However, it was found from the Meteosat reflectivities that the thickest clouds were close to lambertian reflectors while the angular distribution of radiances was more variable for low and intermediate cloudiness. Hence, it should make more sense to parameterise the cloud index - clear sky index relationship with ψ than parameterising the reflectivity of the thickest clouds.

5 Concluding remarks

Heliosat is an algorithm for estimating solar radiation at ground from images taken in the visible range by geostationary satellites. This algorithm consists in principle of two parts: 1) a model to describe the radiation at ground level when there are no clouds, and 2) a method to combine the output of this clear sky model with a measure of the cloud cover to estimate the solar radiation in the general case when there are clouds.

Paper II of this thesis shows a new clear sky model scheme, SOLIS, which is based on a numerical

Radiative Transfer Model, replacing the simple empirical models used earlier. Firstly, this permits the use of more detailed information about aerosols (dust), water vapour and ozone as input, parameters that in the near future will be retrieved operationally using the new generation of the Meteosat satellites. Secondly, the model also provides spectral output which will be useful for deriving specific solar radiation parameters like Ultraviolet radiation, Photosynthetically Active Radiation, Illuminance (visible light) and Solar Cell response. The SOLIS model is seen (in papers II, III and IV) to give reasonable results using climatological input parameters. However, the potential of the scheme can only be released in the near future when operationally retrieved atmospheric parameters are used as input.

Paper III suggests two modifications to the traditional algorithm for calculation of the 'cloud index'. First, a parmeterisation of the effect of non-lambertian reflection from ground makes the algorithm significantly faster and easier to implement. Second, an analytical correction for the radiation scattered from the atmospheric molecules towards the satellite is derived, replacing an empirical expression in the original algorithm. This makes the algorithm more general, and also easier to interpret and develop further. A validation versus ground measurements shows that the accuracy using the new cloud index is similar to using the old one. However, it is also demonstrated how biases which are due to the cloud index and the clear sky model can cancel or add up, and thus it is important that these two separate components of the algorithm are "kept in balance" with each other.

Papers I and IV are validations of several different versions of the Heliosat algorithm. This has given a basis for understanding the algorithm and several corrections and modifications are suggested. Paper V is an assessment of the influence of sub-pixel variability of cloud properties on the reflectance.

6 Bibliography

Beyer H.G.; Costanzo C.; Heinemann D;, 1996: Modifications of the heliosat procedure for irradiance estimates from satellite images, Solar Energy, 56, 207-212.

Cano D; Monget JM;, Albuisson M; Guillard H; Regas N; Wald L;, 1986: A method for the determination of the global solar radiation from meteorological satellite data, Solar Energy, 37, 31-39.

Dumortier, D, 1998: The Satel-Light model of turbidity variations in Europe. Report for the 6th Satel-Light meeting in Freiburg, Germany, September 1998

Dumortier, D, 1995: Modelling global and diffuse horizontal irradiances under cloudless skies with different turbidities. Technical report for the Daylight II project, JOU2-CT92-0144

Fontoynont, M; Dumortier, D; Heinemann, D; Hammer, A; Olseth, J A; Skartveit; Ineichen, P; Reise, C; Page, J; Roche, J; Beyer, H; Wald, L, 1998: Satel-Light: A www server which provides high quality daylight and solar radiation data for western and central Europe. Proc. 9th conference on satellite meteorology and oceanography in Paris, 25-28 May 1998, pp. 434-437

Geiger M.; Diabaté L.; Ménard L.; Wald L., 2002: A Web service for controlling the quality of global solar irradiation, Solar Energy, 73 (6), 475-480.

Gesell, G., 1989: An Algorithm for Snow and Ice Detection Using AVHRR Data: An Extension to the APOLLO Software Package, International Journal of Remote Sensing, 10 (4-5), 897-905.

Grüter, W.; Guillard, H.; Möser, W.; Monget, J-M.; Palz, W.; Raschke, E.; Reinhardt, R.E.; Schwarzmann, P. and Wald, L., 1986: Solar Radiation Data from Satellite Images. Solar Energy R&D in the European Community, Series F, Volume 4, D. Reidel Publishing Company, p. 100

Hammer, A, 2000: Anwendungsspezifische Solarstrahlungsinformationen aus Meteosat-daten, PhD thesis, University of Oldenburg.

Kriebel K. T., Gesell G., Kästner M., Mannstein H, 2003: The cloud analysis tool APOLLO: Improvements and Validation, Int. J. Rem. Sens, 24, 2389-2408.
Kriebel, K.T.; Saunders, R.W.; Gesell, G., 1989: Properties of Clouds Derived from Fully Cloudy AVHRR Pixels, Beiträge zur Physik der Atmosphäre, 62 (3), 165-171.
Lefèvre M.; Bauer, O.; Iehle, A.; Wald, L., 2000: An automatic method for the calibration of time-series of Meteosat images, International Journal of Remote Sensing, 21 (5), 1025-1045.
Leontieva, E; Stamnes, K; Olseth, J A;, 1994: Cloud optical properties at Bergen (Norway) based on the analysis of long-term solar irradiance records, Theoretical and Applied Climatology, 50, 73-82.
Page, J, 1996: Algorithms for the Satel-Light programme. Technical report for the Satel-Light programme
Rigollier C; Bauer O; Wald L;, 2000: On the clear sky model of the 4th European Solar Radiation Atlas with respect to the Heliosat method, Solar Energy, 68(1), 33-48.
Rigollier C.; Lefèvre M.; Blanc Ph.; Wald L., 2002: The operational calibration of images taken in the visible channel of the Meteosat-series of satellites., Journal of Atmospheric and Oceanic Technology, 19 (9), 1285-1293.
Rigollier, C; Lefèvre, M; Wald, L, 2004: The method Heliosat-2 for deriving shortwave solar radiation from satellite images, Solar Energy, 77, 159-169.
Saunders, R.W, 1988: Cloud top temperature/height: A high resolution imagery product from AVHRR data, Meteorological Magazine, 117, 211-221.
Saunders, R.W. and K.T. Kriebel, 1988: An improved method for detecting clear sky and cloudy radiances from AVHRR data, International Journal of Remote Sensing, 9, 123-150.
Scharmer, K;, 1994: Towards a new atlas of solar radiation in Europe, Solar Energy, 15, 81-87.
Taylor, V.R.; Stowe, L.L., 1984: Atlas of reflectance patterns for uniform Earth and cloud surfaces (Nimbus 7 ERB - 61 days). NOAA Technical report NESDIS
Wald, L.; Wald, J-L. and Moussu, G., 1992: A technical note on a low-cost high-quality system for the axquisition and digital processing of images of WEFAX type provided by meteorological geostationary satellites, International Journal of Remote Sensing, 13, 911-916.
Worldwatch Institute, 2003: State of the World 2003, New York: W.W. Norton & Company.
Zelenka A.; Perez R.; Seals R.; Renne D., 1999: Effective accuracy of satellite-derived hourly irradiances, Theor. Appl. Climatol., 62, 199-207.

7 Part II - The papers I-V